JOURNAL OF CATALYSIS 118, 68–78 (1989)

Shape Selectivity in Reactions of Xylenes in Zeolite ZSM–48

RAJIV KUMAR AND PAUL RATNASAMY

National Chemical Laboratory, Pune 411008, India

Received August 2, 1988; revised October 25, 1988

The shape-selective properties of ZSM–48 in the isomerisation of *meta*-xylene and methylation of toluene have been studied and compared with those of other medium-pore zeolites with 10-membered pore openings like ZSM–5, -22, and -23. The shape selectivity of these zeolites in *meta*-xylene isomerisation and methylation of toluene decreases in the order

$$\text{ZSM-22} \approx \text{ZSM-23} > \text{ZSM-48} > \text{ZSM-5}.$$

These differences are explained on the basis of subtle differences in the shape and geometry of their pore and void structures.

INTRODUCTION

Molecular sieve zeolites may be classified, with respect to their shape-selective catalytic properties, broadly into those with 12-, 10-, or 8-membered aluminosilicate pore openings. Zeolites like X, Y, mordenite, and L possess 12-membered rings. ZSM–5, –11, –22, –23, and –48 exemplify zeolites with 10-membered rings and are called medium-pore zeolites. Erionite belongs to the third category with 8-membered rings. In the early years of research in shape selectivity of zeolites, attention was focussed mainly on the differences in shape selectivity between these three categories of zeolites. With the availability, in the eighties, of different zeolites with the same 10-membered pore openings, but different crystallographic structures and shapes of channels, an area of current interest is the more subtle differences in shape selectivity among these latter zeolites. Apart from their intrinsic scientific value, such studies are also of industrial significance since medium-pore zeolites like ZSM–5 are extensively used in many major petroleum and petrochemical processes (xylene isomerisation, toluene disproportionation, production of ethylbenzene, and hydrodewaxing) and availability of other medium-pore zeolites with better shape selectivity will lead to improvements in the abovementioned processes.

The present paper investigates the formation and reactions of xylenes over ZSM–48, a novel, medium-pore zeolite first synthesised by Chu (*1*). The results are compared with those observed in the case of ZSM–5, –22, and –23. ZSM–48 is a high silica zeolite with a disordered structure (2) consisting of ferrierite sheets linked via bridging oxygens located on mirror planes and characterised by ten-ring, non-interpenetrating linear channels whose ideal dimensions are 0.53 × 0.56 nm. The framework topology of ZSM–48 is also possessed by EU–2 (*3*), ZBM–30 (*4*), and EU–11 (*5*). While details of the synthesis of ZSM–48 are known (*1, 5–9*), not much information is available on the catalytic properties of this zeolite, especially in reactions of aromatic hydrocarbons. Jacobs *et al.* (*10, 11*) classified ZSM–48 as a medium-pore zeolite from the product distribution in the conversion of *n*-decane and ethylnonane. Weitkamp *et al.* (*12*) studied the disproportionation of ethylbenzene over a series of zeolites including ZSM–48 and concluded that it possesses 10-membered pore openings. Finally, Chu and Valyocsik (*13*) have recently claimed a process for converting light olefins to gasoline, distillate, and lube range hydrocarbons over it. Neither the

0021-9517/89 $3.00

reactions of xylenes over ZSM-48, nor a comparison of its shape selectivity (in reactions of xylenes) with other medium-pore zeolites has, so far, been reported.

EXPERIMENTAL

Materials. Zeolite ZSM-48 was synthesised using the procedure described in example No. 13 of Ref. (*9*). A solution of 0.78 g $Al_2(SO_4)_3 \cdot 16H_2O$ and 7.2 g hexamethonium dibromide in 60 g of distilled water was added, under stirring, to a solution of 43 g sodium silicate (27.8% SiO_2, 8.2% Na_2O, and 64% H_2O by weight) in 57 g water. Finally, 3.7 g of H_2SO_4 (96–98 wt%) were added very slowly under vigorous stirring. The gel was then transferred to a stainless steel autoclave and crystallisation was carried out at 433 K for 4 days under stirring. After the crystallisation was complete, the contents of the autoclave were quenched with cold water. The crystalline product was filtered, washed thoroughly with deionised water, and dried at 383 K in air overnight.

The catalytically active protonic form of ZSM-48 was obtained as follows: The as-synthesised form was first converted to the sodium form by calcination at 813 K in flowing air for 6 hr to remove the organic matter from the zeolite. This calcined form was then converted to the ammonium form by repeated exchange with NH_4Cl solution (5 *N*). The H-form was obtained by calcination of the ammonium form of ZSM-48 at 813 K for 16 hr in flowing air. The powder so obtained was pelleted, crushed, and sieved to obtain 14–20 mesh particles. 1 g of H-ZSM-48 (on a dry basis) was used in the catalytic experiments. *Meta*-xylene, toluene, and methanol used were of high purity (AnalaR). The procedures for the synthesis of ZSM-5, -22, and -23 have been published earlier (*14–17*).

Procedures. The chemical composition of the zeolites was analysed by a combination of wet chemical, atomic absorption (Hitachi Z-800), and ICP (John Yvon -JY-38 VHR) methods. The zeolites were further characterised by XRD (Philips, PW 1710, CuKα) scanning electron microscopy (Cambridge), DTA/TG (Netsch, Model STA 490) and adsorption techniques. The catalytic activity measurements were carried out in a tubular downflow reactor and the products were analysed by gas chromatography (Shimadzu). Mass balances were routinely calculated for all runs and were found to be better than 97%. The procedures adopted and the apparatus used have been described earlier (*14, 15*).

RESULTS AND DISCUSSION

Physicochemical Characterisation

The SiO_2/Al_2O_3 ratio in H-ZSM-48 was experimentally found to be 160. The XRD pattern of the zeolite (Fig. 1) matched with that published earlier (*3*). The scanning electron micrograph of H-ZSM-48 (Fig. 2) shows the absence of amorphous material. The crystals are in the form of bundles of needles, individual needles being 2–4 μm long and 0.2 μm thick. The XRD and SEM data thus establish the phase purity of the H-ZSM-48 sample used in this study. The synthesis and characterisation of the ZSM-5, ZSM-22, and ZSM-23 zeolites used for comparison purpose are given in our earlier publication (*16*). Their SiO_2/Al_2O_3 ratios were 90, 114, and 110, respectively. The cuboid crystals of ZSM-5 were about 0.3 μm in dimension. ZSM-22 and -23 consisted of fine needle-like crystals of diameter 0.3 μm and length 2 μm. The absence of amorphous matter within the pores of our zeolite samples is indicated by the adsorption data. The adsorption of water, normal and cyclohexanes, and meta-xylene (at 298 K and $P/P_0 = 0.5$) in ZSM-48 was found to be 4.4, 12.3, 4.6, and 7.5 wt%, respectively, to be compared to 2, 4, and 1 wt% for water and normal and cyclohexanes, respectively, reported by Jacobs and Martens (*18*). The specific cyclohexane adsorption volume in ZSM-48 (4.6 wt%) is lower than that in ZSM-5 (5–8

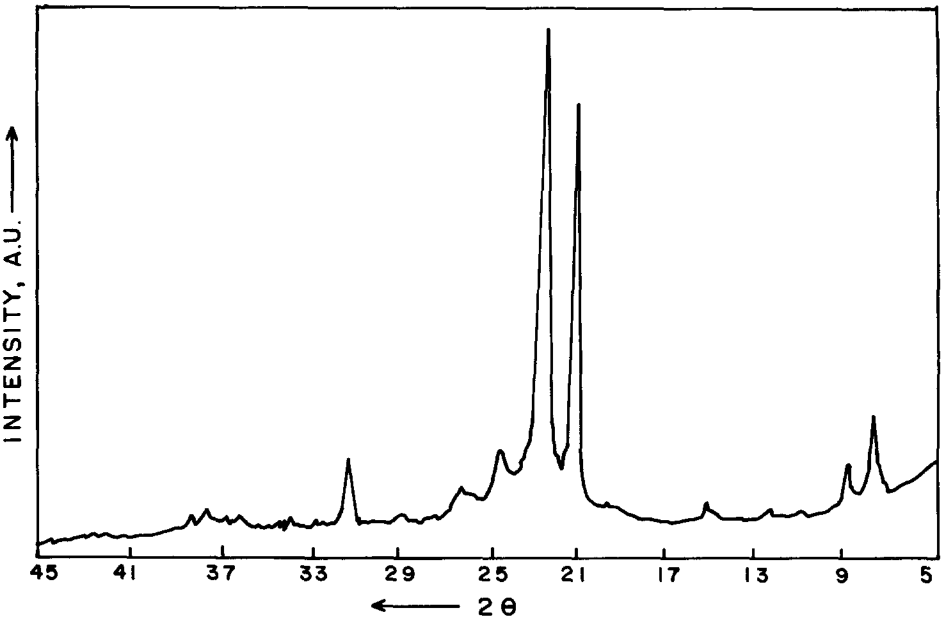

FIG. 1. X-ray diffraction pattern of H-ZSM-48.

wt%). ZSM-22 and -23 adsorbed still less cyclohexane (1.3 and 2.17 wt%, respectively). Though the formal pore size of ZSM-48 very closely resembles that of ZSM-5, the former, unlike the latter, has linear unidimensional channels with no intersections and, hence, is expected to have a smaller accessible internal total pore volume than ZSM-5.

Csicsery (*19*, *20*) had classified shape selectivity effects in catalytic reactions over molecular sieves into three categories:

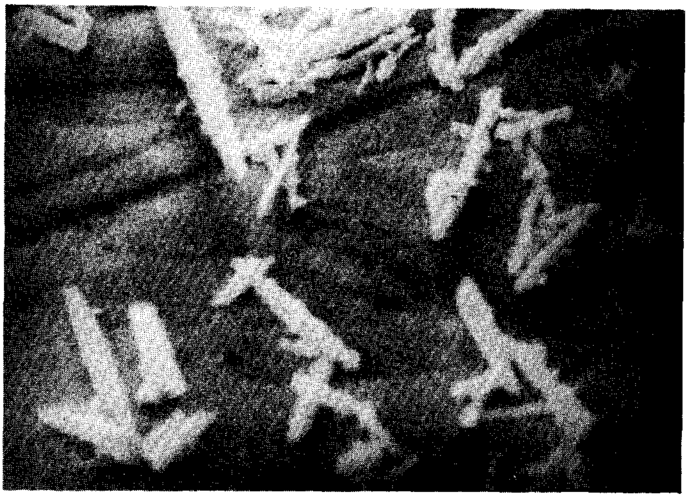

FIG. 2. Scanning electron micrograph of H-ZSM-48.

Those arising from the ability of the zeolite to discriminate differences in the cross-section of [1] the reactants, [2] the products, and [3] the transition-state complex, respectively. Since the former two depend on the relative rates of diffusion of reactants/products during their ingress/egress to and from the active site, they are controlled mainly by the size and shape of the zeolite channels. Transition-state shape selectivity, on the other hand, depends on the void space available around the active site to accommodate transition-state complexes of various dimensions. Bulky transition states (like those involved in the bimolecular disproportionation of xylenes) can form and be accommodated more easily in those medium-pore zeolites that have pore intersections (like ZSM–5) or side-pockets (like EU–1) than in others (like ZSM–22, –23 or –48) that do not have such topological features. Reactions like the intramolecular isomerisation of xylenes pass through transition states that can be accommodated in the 10-ring channels. Hence, the absence of pore intersections and side-pockets in ZSM–48 is expected to enhance the rate of isomerisation vis-à-vis disproportionation (transition-state shape selectivity) of xylenes. These expectations, based on structure and topology, are fully borne out by the results on catalytic properties presented below.

Catalytic Properties: Isomerisation of m-Xylene

In equilibrium reactions in medium-pore zeolites, such as the isomerisation of *meta*-xylene, the relative rates of formation of *para*- and *ortho*-xylenes reflect their diffusionally limited transport and may, hence, form the basis for characterising their pore structure (*21*). In addition to isomerisation, xylene molecules may also undergo transalkylation and dealkylation, the latter especially at high temperatures. The selectivity for isomerisation (equal to the content of *para*- and *ortho*-xylenes in the total reaction products) and the ratio of *ortho*- to *para*-xylenes in the xylene fraction are used, in the present study, as indices of the shape selectivity of ZSM–48.

The influence of temperature and space velocity on product distribution in the isomerisation of *m*-xylene (at a time-on-stream of one hr) over ZSM–48 is shown in Tables 1 and 2. The variation in product distribution due to catalyst aging is shown in Table

TABLE 1

Isomerisation of m-Xylene over H–ZSM–48: Influence of Temperature (Feed: *m*-Xylene + H_2 (1 : 4, mole); WHSV = 3.5 hr^{-1})

Temp. (K)	603	623	643	663	683	703	723
Conversion (%)	8.4	10.0	18.2	26.7	30.6	32.9	35.5
Products (wt%)							
Toluene	0.2	0.2	0.4	0.5	0.6	0.7	1.5
p-Xylene	5.9	7.2	12.9	18.5	21.4	22.2	20.0
m-Xylene	91.6	90.0	81.8	73.3	69.4	67.1	64.5
o-Xylene	2.1	2.4	4.4	7.0	7.8	9.2	12.3
1.3.5 TMB[a]	—	—	—	0.1	0.1	0.1	0.2
1.2.4 TMB[a]	0.2	0.2	0.5	0.6	0.7	0.7	1.3
1.2.3 TMB[a]	—	—	—	—	—	—	0.1
Xyl. loss[b]	0.4	0.4	0.9	1.2	1.4	1.5	3.1
Sel. isom.[c]	0.95	0.96	0.95	0.95	0.95	0.95	0.91
Ortho/Para xyl.	0.35	0.34	0.34	0.38	0.37	0.41	0.61

[a] TMB = Trimethylbenzene.

[b] Xylene loss, wt% = Xylenes in feed – xylenes in product.

[c] Selectivity for xylene isomerisation = [*p*-xyl + *o*-xyl]/*m*-xyl converted.

TABLE 2

Isomerisation of *m*-Xylene over H–ZSM–48: Influence of WHSV (Feed: *m*-Xylene + H_2 (1 : 4, mole); Temp. (K): 683)

WHSV (hr^{-1})	3.5	7	13	17.5
Conversion (%)	30.6	22.5	12.1	7.0
Products (*wt%*)				
Toluene	0.7	0.6	0.2	0.1
p-Xylene	21.4	15.7	8.5	5.0
m-Xylene	69.4	77.5	87.9	93.0
o-Xylene	7.8	5.6	3.2	1.8
1.3.5 TMB[a]	0.1	0.1	—	—
1.2.4 TMB[a]	0.7	0.4	0.2	0.1
Xyl. loss[b]	1.5	1.1	0.4	0.2
Sel. isom.[c]	0.95	0.95	0.97	0.97
Ortho/Para xyl.	0.36	0.36	0.37	0.36

[a,b,c] See Table 1.

3. As the temperature increases, the selectivity for isomerisation remains constant (at 0.95) up to 703 K, beyond which it starts decreasing. The *ortho*/*para* ratio, however, starts increasing beyond 703 K because at higher temperature xylene isomers tend to reach equilibrium concentration. The equilibrium value of the *ortho*/*para* ratio is around 1. The lower the value of this ratio, the greater is the shape selectivity of the zeolite. Similarly, the selectivity for isomerisation would increase with the transition-state shape selectivity of the zeolite. The *ortho*- to *para*-xylene ratio in ZSM–48 is about 0.35 (Table 1). Under similar conditions, ZSM–23 and ZSM–5 exhibit values of 0.24 and 0.74, respectively (*15*, *16*). The three zeolites thus possess shape selectivity in the following decreasing order: ZSM–23 > ZSM–48 > ZSM–5. Values of the selectivity for isomerisation follow a similar trend (0.98, 0.95, and 0.91, respectively). Results of the influence of contact time (Table 2) indicate that while the selectivity for isomerisation increased from 0.95 to 0.97 at low contact time (WHSV = 17.5 hr^{-1}), the *ortho*/*para* ratio remains constant around 0.36. Among the trimethylbenzenes produced by transalkylation, the 1.2.4 isomer with the smallest cross-section is formed in the largest concentration as expected from the shape selectivity of ZSM–48. While ZSM–48 is more shape-selective than ZSM–5 in the isomerisation of xylene, it undergoes deactivation faster than the latter due to coke formation (Table 3). The activity can, however, be fully restored by regeneration in air. As the catalyst ages, the external surface of the

TABLE 3

Isomerisation of *m*-Xylene over H–ZSM–48: Influence of Aging of Catalyst (Feed: *m*-xylene + H_2 (1 : 4, mole); Temp. (K): 683; WHSV: 3.5 hr^{-1})

TOS[a] (hr)	1	2	3	5	8
Conversion (%)	30.6	25.4	23.8	15.7	15.8
Products (*wt%*)					
Toluene	0.7	0.6	0.5	0.2	0.2
p-Xylene	21.4	17.4	16.5	11.3	11.3
m-Xylene	69.4	74.6	76.2	84.3	84.2
o-Xylene	7.8	6.8	6.4	4.0	4.1
1.3.5 TMB[b]	0.1	0.1	0.1	—	—
1.2.4 TMB[b]	0.7	0.5	0.3	0.2	0.2
Xyl. loss[c]	1.5	1.2	0.9	0.4	0.4
Sel. isom.[d]	0.95	0.95	0.96	0.97	0.97
Ortho/Para xyl.	0.36	0.39	0.38	0.35	0.36

[a] TOS = time-on-stream, hr.

[b,c,d] See Table 1.

zeolite crystals wherein most of the transalkylation occurs is covered by a carbonaceous deposit. Hence, as expected, the selectivity for isomerisation increases (Table 3). However, the *ortho*/*para* ratio does not vary to any significant extent. It may be interesting to note that most of the values of the *ortho*/*para* ratio in Tables 1–3 for ZSM–48 fall in the range 0.37 ± 0.02 and seem to be insensitive to changes in reaction parameters like temperature, contact time, and time-on-stream. Similar insensitivity of the *ortho*/*para* ratios to changes in reaction parameters had also been observed by us in the isomerisation of *m*-xylene over ZSM–5, –22, and –23 (*15*, *16*). Dewing (*21*) had shown earlier that this ratio, for a particular zeolite, is insensitive to changes in catalyst parameters like morphology, crystal size, and the distribution of active sites within the crystal. Taking into account both Dewing's and our results, we might state that as long as the *meta*-xylene conversion levels are far from the equilibrium value (say, below 25%), the relative rate of formation of *ortho*- to *para*-xylene is a parameter which defines the shape selectivity of medium-pore zeolites that is dependent only on the crystallographic structure and independent of both morphological features like crystal size and reaction kinetic parameters like temperature and contact time.

Figure 3 illustrates the variation in the selectivity for isomerisation at various conversion levels for ZSM–48. For comparative purpose, the results for ZSM–5, –22, and –23 are also included (*16*). Two features may be noted from Fig. 3. First, the four zeolites may be ranked according to their selectivity for isomerisation of *m*-xylene in the decreasing order: ZSM–22 ≃ ZSM–23 > ZSM–48 > ZSM–5. Second, the decrease in the selectivity for isomerisation with increasing conversion of *m*-xylene is more pronounced for ZSM–5 than for the other three. Even though all the above four zeolites possess 10-membered channels, ZSM–5 differs from ZSM–22, –23, and –48 in one important aspect: The pore system of the ZSM–5 zeolite includes cavities at the intersections of the pores, while those of the latter group consist of non-interpenetrating linear channels with no cavities. More detailed studies are necessary to verify whether this feature can be used to distinguish amongst medium-pore zeolites. Figure 4 illustrates the routes followed in the approach to the equilibrium composition in the isomerisation of *m*-xylene over H–ZSM–48. The results are compared with those of ZSM–5, –22, and

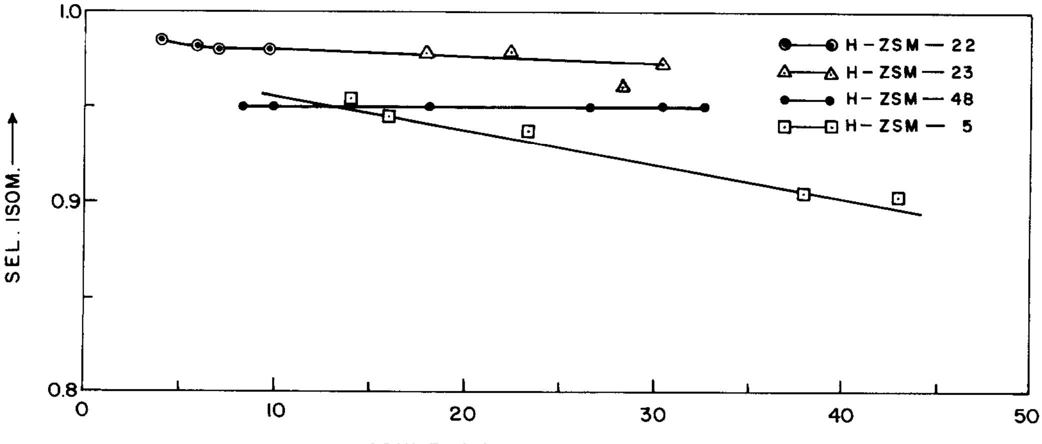

FIG. 3. Variation of the selectivity for xylene isomerisation vs conversion for various zeolites.

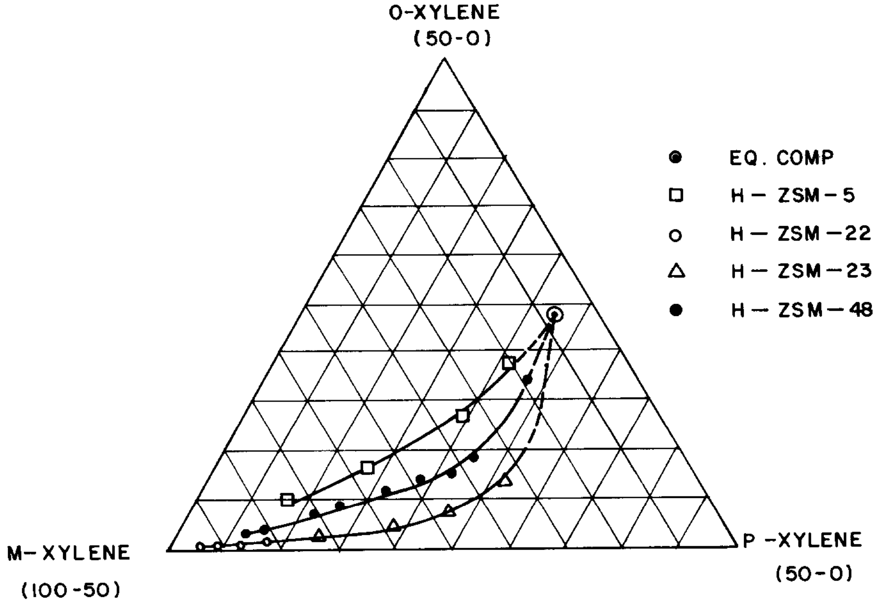

FIG. 4. Approach to equilibrium in xylene isomerisation.

–23 (*16*). The intermediate shape selectivity of ZSM–48, between ZSM–5 on the one hand and ZSM–22 and –23 on the other hand, is clearly evident.

Methylation of Toluene

The methylation of toluene is an electrophilic reaction, the primary products being both *ortho*- and *para*-xylenes. *Meta*-xylene as well as C_9 aromatics are formed by secondary reactions like isomerisation, further alkylation, and transalkylation. Any enrichment of the *para* isomer in the reaction product is due to the product shape selectivity of the catalyst and may be used as an index of the latter provided significant concentration of the secondary products is avoided. This may be seen from Table 4 which illustrates the influence of space velocity on product distribution in the methylation of toluene (time-on-stream = 1 hr) over ZSM–48. At low contact times, the relative concentration of *m*-xylene (among the xylene isomers) decreases whereas that of the *para* isomer increases. As in the case of the products from the reactions of *m*-xylene (Tables 1–3), the concentration of the 1.2.4 isomer is the highest amongst the three trimethylbenzene isomers. An independent study had confirmed that under the

TABLE 4

Methylation of Toluene over H–ZSM–48: Influence of WHSV (Feed: toluene + methanol (4 : 1, mole); Temp. (K): 683)

WHSV (hr^{-1})	3.5	7.0	13.5	17.5
Tol. conv. (%)	18.3	14.4	14.0	7.9
Methanol conv. (%)	100	100	100	99
Products (*wt%*)				
Aliphatics	1.7	1.2	0.9	0.5
Benzene	0.5	0.4	0.2	0.1
Toluene	78.3	82.0	82.3	88.2
p-Xylene	5.8	6.0	6.6	4.4
m-Xylene	6.2	4.7	4.7	3.2
o-Xylene	3.4	2.7	3.0	1.9
p-Ethyltoluene	0.1	—	—	—
m-Ethyltoluene	0.1	—	—	—
1.3.5 TMB[a]	0.5	0.1	0.1	—
1.2.4 TMB[a]	3.0	2.8	2.2	1.6
1.2.3 TMB[a]	0.4	0.1	—	—
Xylenes dist. (%)				
Para-	38	45	46	46
Meta-	40	35	33	34
Ortho-	22	20	21	20

[a] See Table 1.

TABLE 5

Methylation of Toluene over H–ZSM–48: Influence of Temperature (Feed: toluene + methanol (4 : 1, mole); WHSV, hr^{-1}: 3.5)

Temp. (K)	623	643	663	683	703	723
Tol. conv. (%)	5.3	10.2	14.4	18.3	19.2	21.7
Methanol conv. (%)	98	99	100	100	100	100
Products (*wt%*)						
Aliphatics	4.2	3.7	2.1	1.7	1.5	0.4
Benzene	0.3	0.4	0.5	0.5	0.7	0.9
Toluene	90.8	86.0	82.0	78.3	77.4	75.0
p-Xylene	2.2	4.2	5.5	5.8	5.2	5.4
m-Xylene	1.2	2.5	4.5	6.2	7.4	9.3
o-Xylene	1.0	2.0	2.7	3.4	3.2	4.0
p-Ethyltoluene	—	—	—	0.1	0.1	0.1
m-Ethyltoluene	—	—	0.1	0.1	0.1	0.1
1.3.5 TMB[a]	—	—	0.1	0.5	0.6	0.9
1.2.4 TMB[a]	0.3	1.2	2.2	3.0	3.2	3.3
1.2.3 TMB[a]	—	—	0.1	0.3	0.3	0.4
C_{10} aromatics	—	—	0.1	0.1	0.2	0.2
Xylenes dist. (%)						
Para-	50	48	43	38	33	29
Meta-	27	29	35	40	47	50
Ortho-	23	23	22	22	20	21

[a] See Table 1.

experimental conditions of the present study methanol was converted mainly to aliphatic hydrocarbons, mainly olefins, and no aromatics were formed. Hence, the trimethylbenzenes must have been formed from the further reaction of xylenes. The influence of temperature (time-on-stream = 1 hr) is shown in Table 5). While at low temperatures an enrichment in *para*-xylene is observed due to the intrinsic shape selectivity of ZSM–48, its concentration is decreased at higher temperatures due to the further isomerisation of *para*- and *ortho*-xylenes.

In order to confirm that the xylenes are formed only by the methylation of toluene and not by its disproportionation, pure toluene was reacted over H–ZSM–48. Even at high temperatures (783 K), there was practically no reaction taking place; only 1.1–1.7 wt% conversion was obtained, probably on the external surface of the zeolite crystals. This was further supported by the near-equilibrium distribution of the xylene isomers in the product. This indicates that toluene disproportionation, a bimolecular reaction, cannot occur inside the channels of ZSM–48, in sharp contrast to the results obtained in the case of ZSM–5 (*22*), which disproportionated toluene, in significant quantities, to benzene and xylenes. The conversion vs selectivity plots in the methylation of toluene are given in Fig. 5. The relative concentration of the xylene isomers vis-à-vis the equilibrium composition at various levels of toluene conversion are plotted in the triangular composition diagram in Fig. 6. The results of ZSM–5, –22, and –23 (16) are also plotted for purposes of comparison. Once again, the intermediate shape selectivity of ZSM–48 is evident from both the amount of xylenes in the aromatic products and the concentration of *para*-xylene among the xylene isomers.

The above observed differences in shape

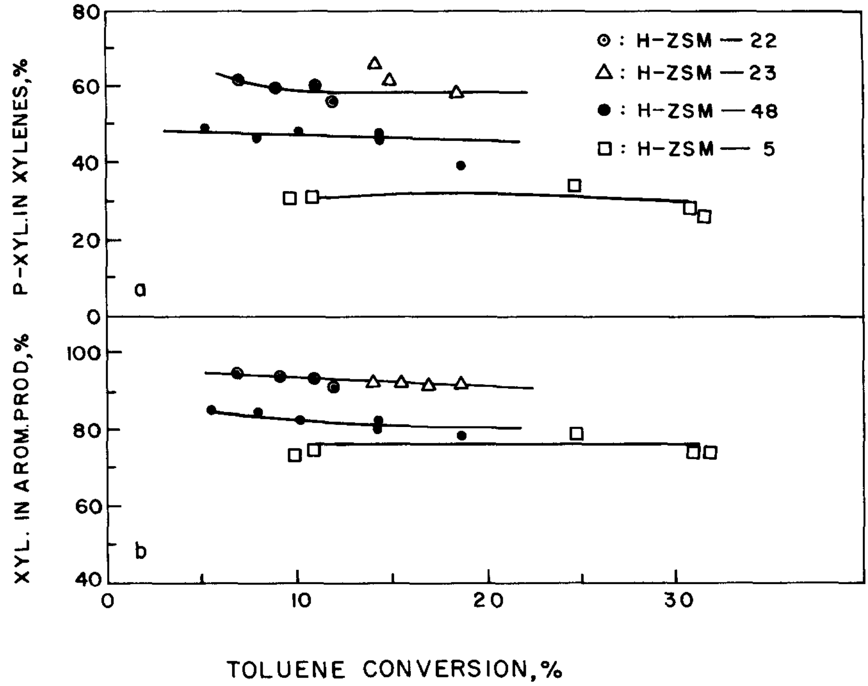

FIG. 5. Influence of conversion level on the concentration of *p*-xylene and total xylenes formed in toluene methylation.

selectivity may be understood from the subtle differences in pore geometry and shape between these four 10-membered ring medium-pore zeolites. In ZSM–5, two types of intersecting channels exist that are both defined by 10-membered oxygen rings. These channels are sinusoidal and parallel to the [100] axis and straight and parallel to

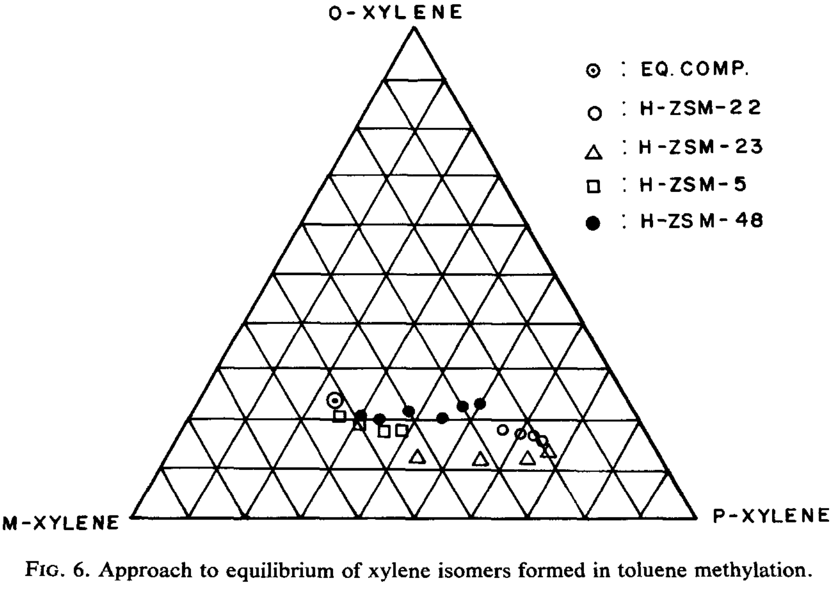

FIG. 6. Approach to equilibrium of xylene isomers formed in toluene methylation.

TABLE 6

Dimensions and Characteristics of Pores in Medium Pore Zeolites

Zeolite	Pore dimension (nm)	Characteristics
ZSM-22	0.55 × 0.45	Unidim, elliptical
ZSM-23	0.56 × 0.45	Unidim, tear drop
ZSM-48	0.53 × 0.56	Unidim, circular
ZSM-5	0.54 × 0.56	Circular; sinusoidal
	0.55 × 0.51	Elliptical; straight; bidim with large intersections

the [010] axis, respectively. The sinusoidal channels are nearly circular with dimensions 0.54 × 0.56 nm, while the straight channels are elliptical with dimensions 0.51 × 0.55 nm. This two-dimensional channel system has pore intersections wherein the cross-section is much larger (about 0.8 nm) and wherein reactions requiring bulky transition states (e.g., xylene disproportionation to toluene and trimethylbenzene) can occur. This is a crucial difference between ZSM-5 and -22, -23, and -48. The latter group possesses one-dimensional nonintersecting channel systems. In ZSM-22, the pores run parallel to the *c* axis and have maximum and minimum free diameters of 0.55 and 0.45 nm, respectively. In ZSM-23, the pore openings have dimensions of 0.56 × 0.45 nm. However, there is a significant difference in the shapes of the pores in ZSM-22 and ZSM-23. While the pores in ZSM-22 are elliptical in shape, those in ZSM-23 are teardrop-shaped. The pore openings in ZSM-48 have dimensions of 0.53 × 0.56 nm. The zeolites are arranged in order of increasing cross-section and void volume in Table 6. From an inspection of Table 6, one would anticipate that shape selectivity would decrease in the order ZSM-22 $\approx$ ZSM-23 > ZSM-48 > ZSM-5, in agreement with results from catalytic experiments presented in this paper.

SUMMARY

The shape-selective properties of H-ZSM-48, a medium-pore 10-membered ring zeolite, in the reactions of *meta*-xylene isomerisation and toluene methylation have been studied and compared with those of other medium-pore zeolites like H-ZSM-22, H-ZSM-23, and H-ZSM-5. In accordance with the effective pore width and presence or absence of channel intersections, the *para*-selectivity, as well as the xylene selectivity in total aromatic products in both the above mentioned reactions follow the order; H-ZSM-22 $\approx$ H-ZSM-23 > H-ZSM-48 > H-ZSM-5.

ACKNOWLEDGMENT

This work was partly funded by UNDP.

REFERENCES

1. Chu, P., U.S. Patent 4,397,827 (1981).
2. Schlenker, J. L., Rohrbaugh, W. J., Chu, P., Valyocsik, E. W., and Kokotailo, G. T., *Zeolites* **5**, 355 (1985).
3. Casci, J. L., Lowe, B. M., and Whittam, T. V., U.K. Pat. Appl. GB 2077709 A (1981).
4. Marosi, L., Schwarzmann, M., and Stebenow, J., Eur. Pat. Appl. No. EPA 0046504 (1982).
5. Araya, A., and Lowe, B. M., *J. Catal.* **85**, 134 (1984).
6. Valyocsik, E. W., U.S. Patent 4,585,747 (1986).
7. Suzuki, K., Kiyozumi, Y., Shin, S., Fujisawa, K., Watanabe, H., Saito, K., and Noguchi, K., *Zeolites* **6**, 290 (1986).
8. Chu, P., U.S. Patent 4,448,675 (1984).
9. Valyocsik, E. W., Eur. Pat. Appl. No. EPA 0142317 (1984).
10. Jacobs, P. A. and Martens, J. A., *in* "New Developments in Zeolite Science and Technology," Proceedings, 7th International Zeolite Conference, Tokyo, 1986 (Y. Murakami *et al.*, Eds.), pp. 23–32. Elsevier, Amsterdam/New York, 1986.
11. Martens, J. A., Tielen, M., Jacobs, P. A., and Weitkamp, J., *Zeolites* **4**, 98 (1984).
12. Weitkamp, J., Ernst, S., Jacobs, P. A., and Karge, H. G., *Erdöl Kohle* **39**, 13 (1986).
13. Chu, C. T., and Valyocsik, E. W., U.S. Patent 4,665,250 (1987).
14. Ratnasamy, P., Babu, G. P., Chandwadkar, A. J., and Kulkarni, S. B., *Zeolites* **6**, 98 (1986).
15. Babu, G. P., Kulkarni, S. B., and Ratnasamy, P., *J. Catal.* **79**, 215 (1983).

16. Kumar, R., and Ratnasamy, P., *J. Catal.*, in press.
17. Babu, G. P., Santra, M., Shiralkar, V. P., and Ratnasamy, P., *J. Catal.* **100,** 458 (1986).
18. Jacobs, P. A., and Martens, J. A., "Synthesis of High-Silica Aluminosilicate Zeolites," p. 289. Elsevier, Amsterdam, 1987.
19. Csicsery, S. M., *Zeolites* **4,** 202 (1984).
20. Csicsery, S. M., *Pure Appl. Chem.* **58,** 841 (1986).
21. Dewing, J., *J. Mol. Catal.* **27,** 25 (1984).
22. Meshram, N. R., Hegde, S. G., Kulkarni, S. B., and Ratnasamy, P., *Appl. Catal.* **8,** 359 (1983).